Absorbing Boundary Condition

FANG Q. HU*

Department of Mathematics and Statistics, Old Dominion University, Norfolk, VA 23529, USA

Absorbing boundary conditions for Computational Aeroacoustics(CAA) are reviewed. Commonly used absorbing zonal techniques, such as sponge layers and buffer zones, as well as Perfectly Matched Layers (PML) are discussed. The basic ideas and central results of these methods are surveyed and summarized. Special attentions will be given to the recently emerged PML technique and its application to CAA. Numerical examples are presented for PML in duct acoustics. A comparison of PML and non-PML absorbing boundary conditions will also be given.

Keywords: Non-reflecting boundary condition; Computational Aeroacoustics; Absorbing boundary condition; Duct acoustics.

1 Introduction

In numerical simulations with an infinite or semiinfinite domain, the open boundaries are necessarily truncated and artificial boundaries are formed. The boundary conditions to be applied at these artificial boundaries should be transparent to out-going disturbances. This turns out to be a difficult problem under most general assumptions and remains an outstanding issue for computational fluid dynamics (CFD) and computational aeroacoustics (CAA). Due to the importance of the subject, there is an extensive literature on non-reflecting boundary conditions. Some previous reviews can be found in Renault(1992), Givoli(1994), Tam(1998), Tsynkov(1998) and Turkel and Yefet(1998).

This paper will review methods that employ "absorbing layers" for the purpose of annihilating the out-going disturbances. In particular, we will focus on methods that are genuinely multi-dimensional and applicable to the Navier-Stokes equations or the Euler equations and leave out absorbing boundary conditions that are primarily for specialized systems such as the wave equation or frequency domain formulations. Special attentions will be given to the recently emerged Perfectly Matched Layer technique and its application to computational aeroacoustics.

In section 2, we will review three commonly used techniques, loosely termed "zonal techniques". The aim here is not to give details of each individual approach, but to survey and summarize the basic ideas and central results of these methods. In section 3, we will discuss the main ideas behind the construction of Perfectly Matched Layers for the linearized Euler equations. The recent work presented in Hu(2001) will be generalized to three dimensional equations and the PML equations are rewritten in a more compact form. Examples of the PML technique for duct acoustics are presented in section 4. We will see that PML is applicable as the inflow and outflow boundary conditions in a ducted environment without a specific modal assumption. Finally, in section 5, we offer a comparison of PML and non-PML absorbing boundary conditions.

2 Zonal techniques

The methods reviewed in this section are variously referred to as "absorbing layers", "sponge layers", "exit zones", or "buffer zones" etc, in the literature. The basic strategy of these methods is to introduce additional zones of grid points, or layers, to surround the truncated physical domain so that out-going disturbances are attenuated in the added zones. The numerical solutions inside absorbing zones need not be physical as long as the use of the zone does not cause significant reflection back into the physical domain. Various ways of constructing the absorbing

 $^{^*}fhu@odu.edu$

zones have been proposed. In this section, we will review three approaches as a representative of what are frequently used in computational fluid dynamics and computational aeroacoustics. We note that these approaches are often implemented in a combined fashion. In some cases, the absorbing zone is terminated with a characteristics based non-reflecting boundary condition (see Hixon(2004) in this special issue) at the exit end of the zone.

2.1 Artificial dissipation and damping

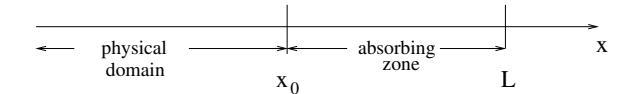


Figure 1: Schematic of an absorbing zone added to the physical domain.

In this approach, an absorbing zone is created and appended to the physical computational domain (Figure 1) in which the governing equations are modified to mimic a physical dissipation mechanism. The advantage of using the physical analogy is that the modified equations will likely be mathematically well-posed. Israeli and Orszag(1981) analyzed the effectiveness of adding artificial dissipation and artificial damping terms to the one dimensional wave equation. Written as a system of two first order equations, the model equations used in their analysis were

$$\frac{\partial v}{\partial t} = \frac{\partial w}{\partial x} + \mu(x) \frac{\partial^2 v}{\partial x^2} - \nu(x)v, \tag{1}$$

$$\frac{\partial w}{\partial t} = \frac{\partial v}{\partial x} \tag{2}$$

where $\mu(x) \geq 0$ and $\nu(x) \geq 0$ were the artificial dissipation and damping coefficients respectively. The $\mu(x)$ term is analogous to the viscous dissipation and the $\nu(x)$ term simulates "Newtonian cooling" or "friction" effects. They analyzed separately the effectiveness of using the μ term and the ν term in an absorbing zone. For example, if the computational domain was $0 \leq x \leq x_0$ and the absorbing zone was created in $x_0 < x \leq L$ with $\mu(x) = \mu_0(constant)$ and v(x) = 0, the reflection coefficient at the interface $x = x_0$ was found to be

$$R = -e^{-2ikx_0} \frac{\alpha - ik \tan[\alpha(L - x_0)]}{\alpha + ik \tan[\alpha(L - x_0)]}$$
(3)

where $\alpha = k/\sqrt{1+i\mu_0 k}$ and k was the wavenumber of the incident wave(Israeli and Orszag(1981)).

Under the assumption that $\mu_0 k \ll 1$, the reflection coefficient was found asymptotically to be

$$|R| \sim e^{-\mu_0 k^2 (L - x_0)} + O(\frac{1}{4}\mu_0 k).$$
 (4)

From (4), it was estimated that to achieve a reflection of 1% by using the μ term alone, an absorbing zone containing at least 15 wavelengths was necessary.

The damping provided by the ν term was found to be more effective. For example, if $\mu(x)=0$ and $\nu(x)=\nu_0(x)$ (with $\nu_0(x_0)=0$) inside the absorbing zone, the formula for the reflection coefficient was given by

$$R = \left| \frac{ikv + v_x}{ikv - v_x} \right|_{x = x_0}$$

It was estimated that minimal reflection might be achieved with a layer of one and a half wavelengths.

The analysis in Israeli and Orszag(1981) also showed that the method can be further improved by using a characteristics based boundary condition or filtering operator at the exit end of the zone.

For the Euler and Navier-Stokes equations, an artificial damping term, such as the ν term in (1), can be easily introduced as follow,

$$\frac{\partial \mathbf{u}}{\partial t} = L(\mathbf{u}) - \nu(\mathbf{u} - \mathbf{u}_0) \tag{5}$$

where ${\bf u}$ is the solution vector and $L({\bf u})$ denotes the spatial operators of the governing equations. Here, ${\bf u}_0$ is the time independent "target" value in the absorbing zone (see Freund(1997)). In Kosloff et al(1986), a system similar to (5) was analyzed for the two-dimensional wave equation, with numerical examples. In particular, the reflection coefficient of a multi-layer absorbing zone was calculated.

2.2 Grid stretching and numerical filtering

Attenuation of the solution may also be achieved by purely numerical means. One such approach, used in Rai et al(1991) and Colonius et al(1993), is to create a "sponge layer", or "exit zone", in which the grids are stretched and coarsened. When an out-going wave enters the sponge layer, it becomes under-resolved in the coarsened grid. Since most numerical schemes have a built-in mechanism of dissipating the disturbances in unresolved scales, the numerical solutions inside the sponge layer are attenuated through numerical dissipation.

Computationally, grid stretching is equivalent to a modification of spatial derivative terms. For example,

if the grids in the x direction are to be stretched, one can replace the x derivative as

$$\frac{\partial}{\partial x} \longrightarrow \frac{1}{\alpha(x)} \frac{\partial}{\partial x}$$
 (6)

where $\alpha(x) \geq 1$ is an increasing function with $\alpha(x_0) = 1$. Then, inside the sponge layer, spatial derivative terms can be discretized in the same way as those in the interior region.

One should be careful that the stretching has to be done very gradually and $\alpha(x)$ must be a slowly varying function, because a sudden increase in grid spacing can cause numerical reflection (e.g., Vichnevetsky(1981) and Hu and Atkins(2002)). This may lead to an excessively large exit zone and sometimes result in an exit zone that has as many grid points as the physical domain. A model of smoothly stretching the grid was discussed in Colonius et al(1993).

The attenuation of the numerical solution, however, can be enhanced by applying low-pass numerical filters inside the added zone, thus reducing the length of the exit zone. In Colonius et al(1993), a five-point explicit filter operation was enforced in the sponge layer. In Visbal and Gaitonde (2001), implicit high-order filters were used. It was noted in Visbal and Gaitonde(2001) that, since grid stretching could cause high frequency grid-to-grid oscillations, highorder filters should be applied to the solutions in the physical domain as well. Examples were presented in Visbal and Gaitonde(2001) where grid stretching could even be done non-smoothly when combined with high-order filters. In Liu et al(1993), a grid stretching in the streamwise direction was combined with an increase in viscous dissipation similar to the μ term in (1) in section 2.1.

Another technique of creating an absorbing zone is to directly multiply the disturbances with an appropriate damping function. In Wasistho et al(1997), the numerical solution inside the absorbing zone is modified, at each Runge-Kutta stage, according to the following formula,

$$\mathbf{u} = \mathbf{u}_{ref} + \xi(x)(\mathbf{u} - \mathbf{u}_{ref})$$

where \mathbf{u}_{ref} is a reference "target" flow and $\xi(x)$ is a smooth function that varies from unity, at the start of the absorbing zone, to zero, at the end of the zone. This approach was shown to be effective for absorbing the Tollmien-Schlichting wave in a compressible boundary layer. Details on the formulation of the damping function $\xi(x)$ were given in Wasistho et al(1997).

2.3 Modification of convective mean velocity

In numerical simulations of laminar to turbulent transitions of incompressible flows, it was recognized that the upstream influence of an outflow boundary resulted from the ellipticity of the Navier-Stokes equations (see Streett and Macaraeg(1989)). To eliminate the upstream influence, a buffer zone was introduced in Streett and Macaraeg(1989) in which the viscous effects were gradually reduced to zero and the governing equations were modified to be completely hyperbolic with an outward convective mean flow, thus forgoing the necessity of non-reflecting boundary conditions. This method of modifying the characteristics of the governing equations has been extended to compressible Euler equations and Navier-Stokes equations in the works by Ta'asan and Nark(1995) and Freund(1997). In Ta'asan and Nark(1995), for the compressible Euler equations, the mean flow inside the buffer zone was modified to increase gradually and become eventually supersonic at the end of the buffer domain. At that point, since the flow is supersonic and outward, termination of the grid will not cause any reflection. In Freund(1997), this approach was combined with additional damping terms similar to those used in a sponge layer. The combination was shown in numerical simulations to be effective in reducing the length of the buffer zone and work better than stand-alone characteristics-based boundary conditions for the Navier-Stokes equations. The buffer zone was also used to impose inflow boundary condition in Freund(1997).

The formulation and implementation of the buffer zone appears to be relatively simple. It essentially involves an addition to the governing equations of artificial convective terms of the form

$$U_0(x,y)\frac{\partial \mathbf{u}}{\partial x} + V_0(x,y)\frac{\partial \mathbf{u}}{\partial y}$$

where U_0 and V_0 are the artificial velocities that are zero at the start of the buffer zone and are gradually increased to become supersonic in the outward direction.

In all the methods reviewed above, the performance of the absorbing zone depends largely on the gradualness in the variation of the added absorbing terms, the length of the absorbing zone as well as the wavelength of the out-going disturbances. The issue then is computational efficiency. In the next section, a method for the linearized Euler equations, based on the Perfectly Matched Layer technique, will be reviewed where the absorbing zone can be significantly shortened. A heuristic argument about the difference

between the Perfectly Matched Layer and the zonal techniques will be discussed in section 5.

3 Perfectly Matched Layers

The Perfectly Matched Layer (PML) technique was first proposed in Berenger (1994) for numerical solution of Maxwell equations. It showed for the first time that it was possible to formulate an absorbing layer that was theoretically reflectionless for electromagnetic waves of any frequency and any angle of incidence. PML quickly became the method of choice in the computational electromagnetics community. The extension of the PML technique to the Euler equations was first given in Hu(1996a,b). However, it was found that a direct adaption of the split formulation of Berenger (1994) to the Euler equations can give rise to instabilities in the PML domain (e.g., Hu(1996a), Abarbanel et al(1997), Tam et al (1998) and Hesthaven(1998)). Recently, a new formulation of a Perfectly Matched Layer for the Euler equations was proposed in Hu(2001). The new formulation eliminated the instability waves of Hu(1996a) while still being perfectly matched to the linearized Euler equations. Similar ways of avoiding instability in the PML domain were also discussed in several recent works, e.g., Becache et al(2003) and Hagstrom et al(2003). In this section, we will review the main ideas of constructing stable Perfectly Matched Layers for Euler equations. In the next section, examples for duct acoustics will be given.

3.1 Basic ideas of PML

We will illustrate the basic ideas for the PML technique through the construction of a vertical x-layer for the linearized Euler equations with a constant mean flow. Let the governing equations be written as

$$\frac{\partial \mathbf{u}}{\partial t} + \mathbf{A} \frac{\partial \mathbf{u}}{\partial x} + \mathbf{B} \frac{\partial \mathbf{u}}{\partial y} = 0 \tag{7}$$

where

$$\mathbf{u} = \begin{pmatrix} \rho \\ u \\ v \\ p \end{pmatrix}, \ \mathbf{A} = \begin{pmatrix} M & 1 & 0 & 0 \\ 0 & M & 0 & 1 \\ 0 & 0 & M & 0 \\ 0 & 1 & 0 & M \end{pmatrix},$$

$$\mathbf{B} = \begin{pmatrix} 0 & 0 & 1 & 0 \\ 0 & 0 & 0 & 0 \\ 0 & 0 & 0 & 1 \\ 0 & 0 & 1 & 0 \end{pmatrix}. \tag{8}$$

Here, ρ is the density, (u, v) is the velocity vector, p is the pressure, and M is the Mach number of the mean flow.

As shown in previous works for the Maxwell equations, e.g., Chew et al(1994), Gedney(1996), Zhao et al(1996), Collino et al(1998), Petropoulos(2000) and Turkel et al(1998), the PML technique can be viewed as a complex change of variables in the frequency domain. However, to avoid generating instability waves in the PML domain, it has been found necessary to introduce a coordinate transformation before applying the PML technique. It was suggested in Hu(2001) that the following transformation be made,

$$\bar{x} = x, \ \bar{y} = \sqrt{1 - M^2}y, \ \bar{t} = t + \frac{M}{1 - M^2}x.$$
 (9)

In the transformed variables \bar{x} , \bar{y} and \bar{t} , the linearized Euler equation (7) is written as

$$\left(\mathbf{I} + \frac{M}{1 - M^2}\mathbf{A}\right)\frac{\partial \mathbf{u}}{\partial \bar{t}} + \mathbf{A}\frac{\partial \mathbf{u}}{\partial \bar{x}} + \sqrt{1 - M^2}\mathbf{B}\frac{\partial \mathbf{u}}{\partial \bar{y}} = 0$$
(10)

where I is the identity matrix. In the frequency domain, equation (10) becomes

$$-i\bar{\omega}\left(\mathbf{I} + \frac{M}{1 - M^2}\mathbf{A}\right)\hat{\mathbf{u}} + \mathbf{A}\frac{\partial\hat{\mathbf{u}}}{\partial\bar{x}} + \sqrt{1 - M^2}\mathbf{B}\frac{\partial\hat{\mathbf{u}}}{\partial\bar{y}} = 0$$
(11)

where we have assumed $\mathbf{u}(\bar{x}, \bar{y}, \bar{t}) = e^{-i\bar{\omega}\bar{t}}\hat{\mathbf{u}}(\bar{x}, \bar{y}).$

At this point, a key step is a complex change of variable for \bar{x} as follows,

$$\bar{x} \longrightarrow \bar{x} + \frac{i}{\bar{\omega}} \int_{\bar{x}_0}^{\bar{x}} \sigma_x dx$$
 (12)

where $\sigma_x(x)>0$ is the absorption coefficient and \bar{x}_0 is the coordinate at the start of the PML domain. Here, σ_x can be constant (as in Hu(2001)) or any spatially varying function. The change of variable (12) will be referred to as the PML complex change of variable in this paper. Accordingly, the partial derivative $\frac{\partial}{\partial \bar{x}}$ will be modified as

$$\frac{\partial}{\partial \bar{x}} \longrightarrow \frac{1}{1 + \frac{i\sigma_x}{\bar{\phi}}} \frac{\partial}{\partial \bar{x}}$$

and equation (11) becomes

$$-i\bar{\omega}\left(\mathbf{I} + \frac{M}{1 - M^2}\mathbf{A}\right)\hat{\mathbf{u}} + \frac{1}{1 + \frac{i\sigma_x}{\bar{\omega}}}\mathbf{A}\frac{\partial\hat{\mathbf{u}}}{\partial\bar{x}}$$
$$+\sqrt{1 - M^2}\mathbf{B}\frac{\partial\hat{\mathbf{u}}}{\partial\bar{y}} = 0. \tag{13}$$

This is the PML equation in the frequency domain.

Equation (13) can be written back in the time domain in several different ways. One way, without splitting the equations or the physical variables, is to multiply the equation by $(1+\frac{i\sigma_x}{\bar{\omega}})$ which gives immediately

$$\left(\mathbf{I} + \frac{M}{1 - M^2}\mathbf{A}\right)\left(-i\bar{\omega}\mathbf{u} + \sigma_x\hat{\mathbf{u}}\right) + \mathbf{A}\frac{\partial\hat{\mathbf{u}}}{\partial\bar{x}}$$

$$+\sqrt{1-M^2}\mathbf{B}\frac{\partial\hat{\mathbf{q}}}{\partial\bar{y}} + \sigma_x\sqrt{1-M^2}\mathbf{B}\frac{\partial\hat{\mathbf{q}}}{\partial\bar{y}} = 0 \qquad (14)$$

where $\hat{\mathbf{q}}$ is an auxiliary variable and defined as

$$\hat{\mathbf{q}} = \frac{i}{\bar{\omega}} \hat{\mathbf{u}}.$$

The time domain version can be readily obtained from (14). When expressed in the original variables x, y and t, we get the following set of equations to be used in a vertical PML domain,

$$\frac{\partial \mathbf{u}}{\partial t} + \mathbf{A} \frac{\partial \mathbf{u}}{\partial x} + \mathbf{B} \frac{\partial \mathbf{u}}{\partial y} + \sigma_x \mathbf{B} \frac{\partial \mathbf{q}}{\partial y} + \sigma_x \mathbf{u} + \frac{\sigma_x M}{1 - M^2} \mathbf{A} \mathbf{u} = 0,$$
(15)

$$\frac{\partial \mathbf{q}}{\partial t} = \mathbf{u}.\tag{16}$$

Similarly, for problems where both the vertical and horizontal absorbing layers (including corners) are needed, the PML complex change of variable should be applied to both \bar{x} and \bar{y} ,

$$\bar{x} \longrightarrow \bar{x} + \frac{i}{\bar{\omega}} \int_{\bar{x}_0}^{\bar{x}} \sigma_x dx, \qquad \bar{y} \longrightarrow \bar{y} + \frac{i}{\bar{\omega}} \int_{\bar{y}_0}^{\bar{y}} \sigma_y dy$$

where σ_x and σ_y are functions of x and y respectively. This leads to a PML equation for the 2-D Euler equations as follows,

$$\frac{\partial \mathbf{u}}{\partial t} + \mathbf{A} \frac{\partial \mathbf{u}}{\partial x} + \mathbf{B} \frac{\partial \mathbf{u}}{\partial y} + \sigma_y \mathbf{A} \frac{\partial \mathbf{q}}{\partial x} + \sigma_x \mathbf{B} \frac{\partial \mathbf{q}}{\partial y} + (\sigma_x + \sigma_y) \mathbf{u}$$

$$+\sigma_x \sigma_y \mathbf{q} + \frac{\sigma_x M}{1 - M^2} \mathbf{A} (\mathbf{u} + \sigma_y \mathbf{q}) = 0.$$
 (17)

where \mathbf{q} is the same as in (16)(see $\mathrm{Hu}(2001)$).

We note that equation (17) recovers the Euler equation (7) when $\sigma_x = \sigma_y = 0$. Since σ_x and σ_y are functions of x and y respectively, it follows that, in a vertical x-layer, σ_x is non-zero but $\sigma_y = 0$; in a horizontal y-layer, σ_y is non-zero but $\sigma_x = 0$; in the corner layer, both σ_x and σ_y are non-zero, as illustrated in Figure 2. Equation (17) has been shown to be perfectly matched to the Euler equation (7). That is, theoretically no reflection will occur when

an acoustic, vorticity or entropy wave enters the PML domain from the Euler domain, regardless of the wave frequency and angle of propagation. Once entered the PML domain, the amplitude of the wave decays exponentially.

Furthermore, the auxiliary variable \mathbf{q} is only needed inside the PML domains, because the spatial derivative $\frac{\partial \mathbf{q}}{\partial x}$ is only required when $\sigma_y \neq 0$ which only happens inside a horizontal y-layer or corner layer and $\frac{\partial \mathbf{q}}{\partial y}$ is only required when $\sigma_x \neq 0$ inside a vertical x-layer or corner layer. As a result, we do not need to compute nor store \mathbf{q} in the Euler domain.

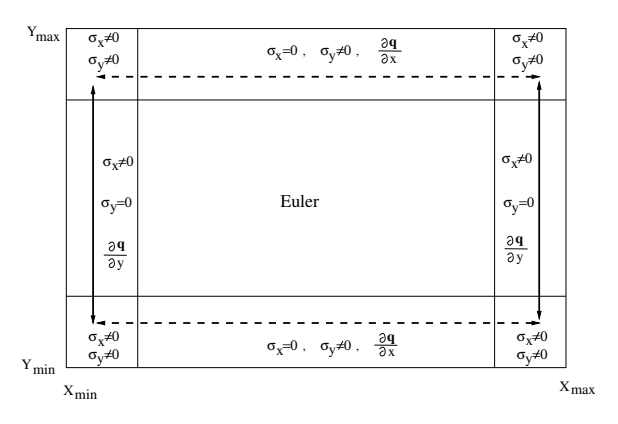


Figure 2: Illustration of a computational domain combining the Euler and PML domains. Solid arrowed lines indicate the domains where $\partial \mathbf{q}/\partial y$ is needed and dashed arrowed lines indicate the domains where $\partial \mathbf{q}/\partial x$ is needed.

Equation (17) can be conveniently written in a compact form that resembles the original Euler equations as follows,

$$\frac{\partial \mathbf{u}}{\partial t} + \mathbf{A} \frac{\partial \mathbf{u}^y}{\partial x} + \mathbf{B} \frac{\partial \mathbf{u}^x}{\partial y} + \mathbf{u}^* + \frac{\sigma_x M}{1 - M^2} \mathbf{A} \mathbf{u}^y = 0$$
(18)

where

$$\mathbf{u}^y = \mathbf{u} + \sigma_y \mathbf{q}, \ \mathbf{u}^x = \mathbf{u} + \sigma_x \mathbf{q},$$

and
$$\mathbf{u}^* = (\sigma_x + \sigma_y)\mathbf{u} + \sigma_x\sigma_y\mathbf{q}$$

The absorbing coefficients are often taken to be power functions, for example,

$$\sigma_x(x) = \sigma_m \left| \frac{x - x_0}{D} \right|^{\beta} \tag{19}$$

or exponential functions, for example,

$$\sigma_x(x) = \sigma_m (1 - e^{-\delta[(x - x_0)/D]^2})$$

where D is the thickness of the PML domain and δ is a parameter controlling the rate of change of $\sigma_x(x)$.

3.2 PML for 3-D Euler equations

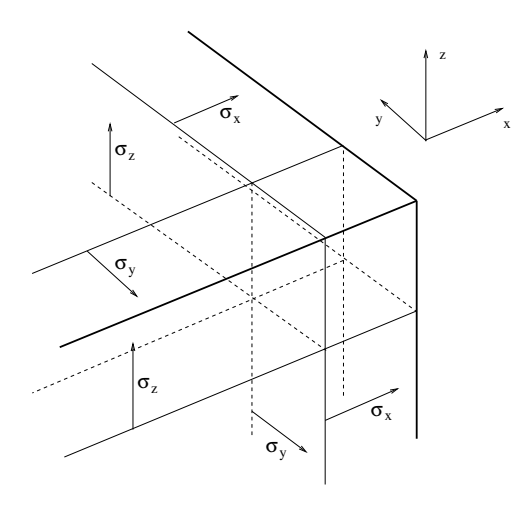


Figure 3: Schematic of PML domains in three dimension.

The PML technique can be applied to the Euler equations in three dimensions as shown in Hu(2002). Let the linearized Euler Equations be written in the matrix form as

$$\frac{\partial \mathbf{u}}{\partial t} + \mathbf{A} \frac{\partial \mathbf{u}}{\partial x} + \mathbf{B} \frac{\partial \mathbf{u}}{\partial y} + \mathbf{C} \frac{\partial \mathbf{u}}{\partial z} = 0 \tag{20}$$

where A, B and C are matrices with constant coefficients.

After applying the transformation

$$\bar{x} = x, \ \bar{y} = \sqrt{1 - M^2}y, \ \bar{z} = \sqrt{1 - M^2}z,$$

$$\bar{t} = t + \frac{M}{1 - M^2}x$$

and the PML complex change of variables to the transformed equation,

$$\bar{x} \longrightarrow \bar{x} + \frac{i}{\bar{\omega}} \int_{\bar{x}_0}^{\bar{x}} \sigma_x dx, \qquad \bar{y} \longrightarrow \bar{y} + \frac{i}{\bar{\omega}} \int_{\bar{y}_0}^{\bar{y}} \sigma_y dy,$$

$$\bar{z} \longrightarrow \bar{z} + \frac{i}{\bar{\omega}} \int_{\bar{z}_0}^{\bar{z}} \sigma_z dz,$$

we get the PML equations in 3-D,

$$\frac{\partial \mathbf{u}}{\partial t} + \mathbf{A} \frac{\partial \mathbf{u}^{yz}}{\partial x} + \mathbf{B} \frac{\partial \mathbf{u}^{xz}}{\partial y} + \mathbf{C} \frac{\partial \mathbf{u}^{xy}}{\partial z} + \mathbf{u}^* + \frac{\sigma_x M}{1 - M^2} \mathbf{A} \mathbf{u}^{yz} = 0$$
(21)

where

$$\mathbf{u}^{yz} = \mathbf{u} + (\sigma_y + \sigma_z)\mathbf{q}_1 + \sigma_y\sigma_z\mathbf{q}_2,$$

$$\mathbf{u}^{xz} = \mathbf{u} + (\sigma_x + \sigma_z)\mathbf{q}_1 + \sigma_x\sigma_z\mathbf{q}_2,$$

$$\mathbf{u}^{xy} = \mathbf{u} + (\sigma_x + \sigma_y)\mathbf{q}_1 + \sigma_x\sigma_y\mathbf{q}_2,$$

$$\mathbf{u}^* = (\sigma_x + \sigma_y + \sigma_z)\mathbf{u} + (\sigma_y \sigma_z + \sigma_x \sigma_z + \sigma_x \sigma_y)\mathbf{q}_1 + \sigma_x \sigma_y \sigma_z \mathbf{q}_2$$

and the auxiliary variables \mathbf{q}_1 and \mathbf{q}_2 are computed as

$$\frac{\partial \mathbf{q}_1}{\partial t} = \mathbf{u},\tag{22}$$

$$\frac{\partial \mathbf{q}_2}{\partial t} = \mathbf{q}_1. \tag{23}$$

The absorption coefficients σ_x , σ_y and σ_z are functions of x, y and z respectively, as illustrated in Figure 3. Again, it is easy to verify that the auxiliary variables \mathbf{q}_1 and \mathbf{q}_2 are only required inside the added PML domains and need not be known inside the Euler domain. Obviously, equation (21) can be further simplified wherever any of the absorption coefficients is zero. In particular, \mathbf{q}_2 is not needed in a region where any two of the absorption coefficients are zero.

3.3 Termination of PML domain and effectiveness of PML

Although PML is theoretically reflectionless, the PML domain in actual computation is of finite length and a certain boundary condition has to be applied to terminate the PML domain itself (Figure 2). The main consideration here is to maintain numerical stability and to use boundary conditions that are consistent with the stability requirements of the numerical scheme. Reflections that occur at the outer boundaries do not really concern us because when the outgoing waves reach the PML outer boundary, their magnitudes have already been reduced significantly and are usually exponentially small. Even when they are reflected, these waves will travel through the PML domain again and be damped further before they reenter the physical domain.

Several types of boundary conditions are possible. One possibility is to use a set of simple boundary conditions as suggested in Hu(2001), i.e.,

at
$$x = X_{max}, y = Y_{min}$$
 and $y = Y_{max}$: $p = 0$,
at inflow $x = X_{min}$: $p = \rho = v = 0$,

in which $[X_{min}, X_{max}] \times [Y_{min}, Y_{max}]$ denotes the entire computational domain as indicated in Figure 2. The second possibility is to apply other non-reflecting boundary conditions such as the characteristics-based non-reflecting boundary conditions. The third possibility is to apply periodic boundary conditions when two opposite sides of the computational domain are covered by PML absorbing layers as in Hu(1996a) and Alpert et al(2002).

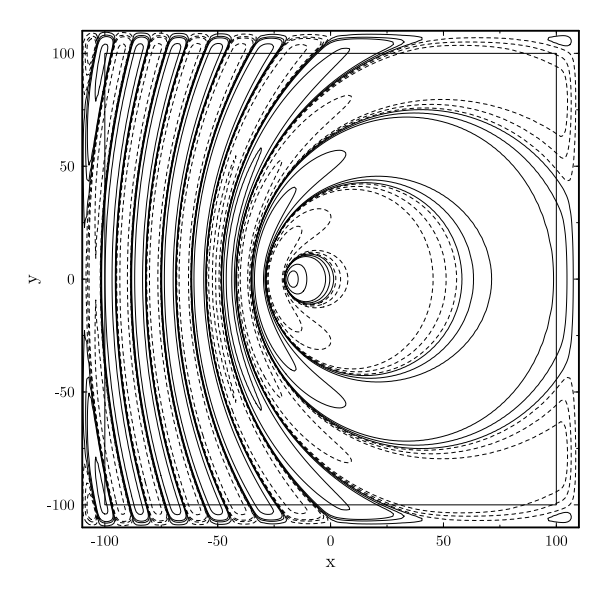


Figure 4: Contours of the pressure p at levels ± 0.1 , ± 0.05 , ± 0.01 , ± 0.005 and ± 0.001 . M=0.8, $D=10\Delta x$. t=600.

To estimate the efficiency of a finite length PML domain, consider a plane acoustic wave incident on the vertical x-layer (where $\sigma_y = 0$). The transmitted wave inside the PML domain has been found to be of the form

$$\hat{\mathbf{u}} = A\hat{\mathbf{e}}_a exp(\frac{i\omega\cos\phi}{1 + M\cos\phi}x$$

$$-\frac{M+\cos\phi}{(1-M^2)(1+M\cos\phi)}\int_{x_0}^x \sigma_x dx + \frac{i\omega\sin\phi}{1+M\cos\phi}y$$
(24)

where $\hat{\mathbf{e}}_a$ is the eigenvector of the acoustic wave and A an arbitrary constant(Hu(2001)). Here ϕ is the angle of the phase plane. Assuming a prefect reflection at the end of the PML domain of thickness D, the reflected wave travels through the PML domain again and, when it re-enters the Euler domain, the original wave amplitude is reduced by a factor of the reflection coefficient R,

$$R = exp(-\frac{2\cos\phi}{1 - M^2\cos^2\phi} \int_{x_0}^{x_0 + D} \sigma_x dx).$$
 (25)

For σ_x in the form of (19), the theoretical reflection coefficient is

$$R = exp(-\frac{2\cos\phi}{1 - M^2\cos^2\phi} \frac{\sigma_m D}{\beta + 1}). \tag{26}$$

From (26), we see that the reflection coefficient reduces exponentially with D and σ_m . Furthermore, R is independent of the frequency, or the wavelength, of the out-going wave.

The reflection coefficient R can be further reduced if we combine the PML with a grid stretching of the form (6), e.g., Petropoulos(2000) and Zhao et al(1996). Then, the reflection coefficient will be

$$R = exp(-\frac{2\cos\phi}{1 - M^2\cos^2\phi} \int_{x_0}^{x_0 + D} \alpha(x)\sigma_x dx)$$

where $\alpha(x) \geq 1$ is the stretching factor.

A numerical example given in Hu(2001) is replotted in Figure 4, where the Euler equations were solved with the following source term added to the equation for the pressure:

$$P(x, y, t) = \sin(\Omega t)e^{-(\ln 2)\frac{(x+20)^2 + y^2}{9}}.$$

The frequency of the source is $\Omega=0.03\pi$ and the mean flow Mach number is M=0.8. Due to the mean flow, the acoustic wave has a larger wavelength at the downstream boundary than that at the upstream boundary. The Euler equations are solved in the square domain $[-100,100]\times[-100,100]$. The PML domains for this calculation have a thickness $D=10\Delta x$. Pressure contours of the numerical solution at t=600 are plotted in Figure 4. This example shows that PML equations can be effective for absorbing long as well as short waves.

4 Ducted Environment

The PML absorption boundary condition discussed in the previous section can be readily used to terminate an open boundary inside a duct. In fact, in a confined environment, the PML equation is simpler because it is only necessary to apply the absorbing boundary condition in one direction.

4.1 PML absorbing condition for duct acoustics

Consider a duct with rigid walls and a rectangular cross section, shown in Figure 5(top). Suppose that

the physical domain is to be terminated at x = A and x = B in the inflow and outflow boundaries respectively. To absorb the out-going waves at these artificial boundaries, we add vertical x-layers. The PML equations to be used in the added domains involve only σ_x ,

$$\frac{\partial \mathbf{u}}{\partial t} + \mathbf{A} \frac{\partial \mathbf{u}}{\partial x} + \mathbf{B} \frac{\partial \mathbf{u}^x}{\partial y} + \mathbf{C} \frac{\partial \mathbf{u}^x}{\partial z} + \mathbf{u}^* + \frac{\sigma_x M}{1 - M^2} \mathbf{A} \mathbf{u} = 0$$
(27)

where

$$\mathbf{u}^x = \mathbf{u} + \sigma_x \mathbf{q}_1 \text{ and } \mathbf{u}^* = \sigma_x \mathbf{u}$$

and \mathbf{q}_1 is the same as that in equation (22). This, of course, is just a special case of (21) with $\sigma_y = \sigma_z = 0$.

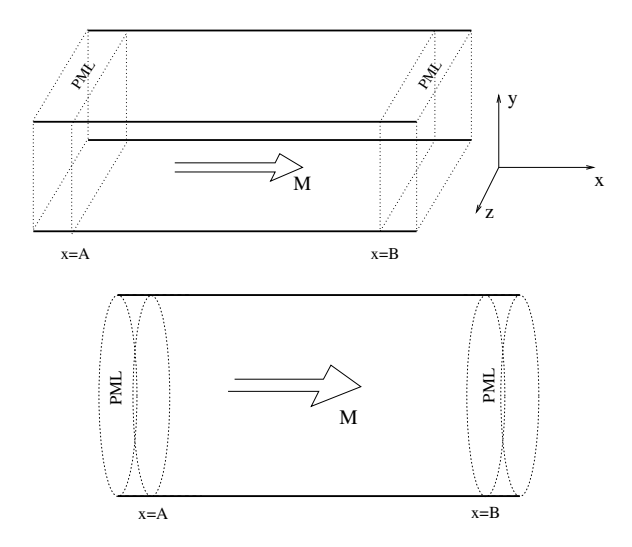


Figure 5: Schematic of a rectangular duct in three dimensions. Top: rectangular duct; bottom: circular duct.

We show the numerical solution of an acoustic pulse inside a two-dimensional duct. The mean flow has a Mach number M=0.5. The entire computational domain is $[-110,110]\times[-50,50]$ where solid walls are located at $y=\pm 50$. A uniform grid of $\Delta x=\Delta y=1$ has been used. The PML domain has a thickness of $10\Delta x$. The acoustic pulse is initiated at t=0 by the initial condition:

$$\rho = u = v = 0, p = e^{-(\ln 2)\frac{(x+50)^2+y^2}{6^2}}$$

Figures 6(a)-(c) show the pressure contours inside the duct at t = 60,110 and 150. As the acoustic pulse is convected downstream, it is reflected by the duct walls. However, no visible reflection from the

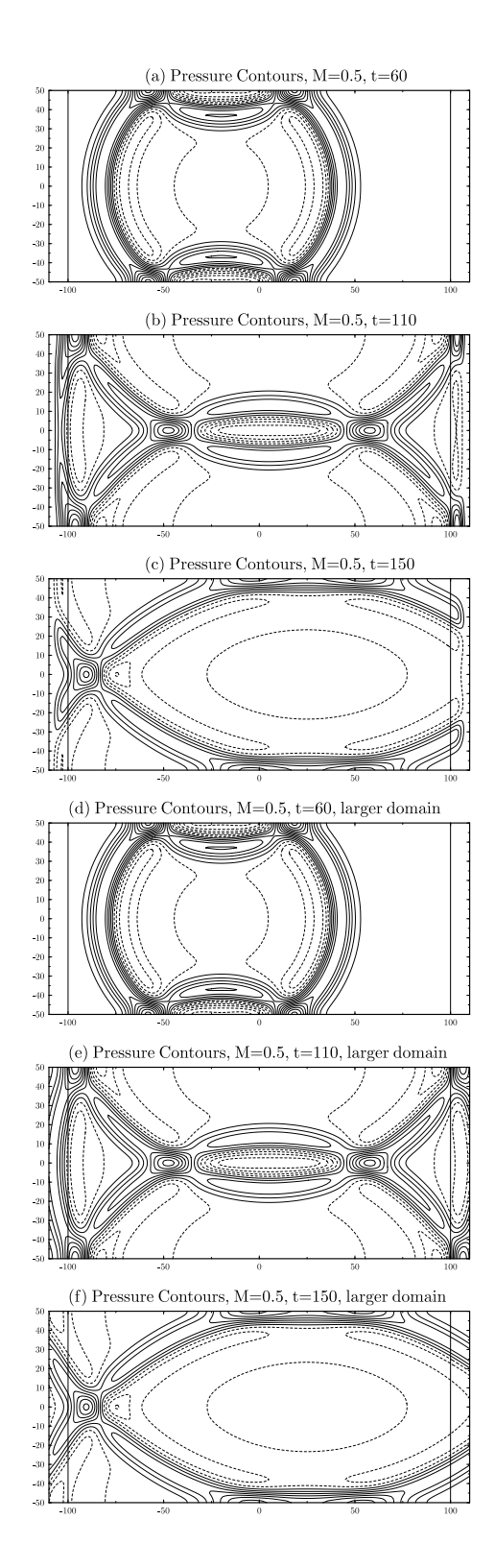


Figure 6: Propagation of an acoustic pulse inside a 2-D duct with solid walls. $M=0.5, D=10\Delta x$. (a)-(c): numerical solution; (d)-(f): reference solution with a larger domain. Vertical lines at $x=\pm 100$ indicate the start of PML domains.

open boundaries is detected. For comparison, a reference solution with a larger domain is plotted in Figures 6(d)-(f). This example shows that PML can be an effective non-reflecting boundary for duct acoustics without assuming any specific modal form of the acoustic waves.

4.2 Use of PML as inflow condition

In many duct acoustics problems, an incoming wave is to be specified at the inflow boundary. The PML technique can be used to impose the incoming waves. Inside the PML domain for the inflow boundary, there are both the incoming and out-going waves. The left-traveling out-going waves in the inflow region can be a result of reflections occurred inside the duct (e.g., a nonuniform duct) or at the out-flow boundary. It is the out-going waves that are to be absorbed. The incoming wave, on the other hand, should not be modified at all. This can be achieved as follows. Since the incoming wave is known, we compute the physical variables in the inflow PML domain as a sum of two parts:

$$\mathbf{u} = \mathbf{u}_{inc} + \mathbf{u}' \tag{28}$$

where \mathbf{u}_{inc} denotes the specified incoming wave and \mathbf{u}' is the part representing the out-going wave. The PML equation (27) is then applied to advance \mathbf{u}' in time.

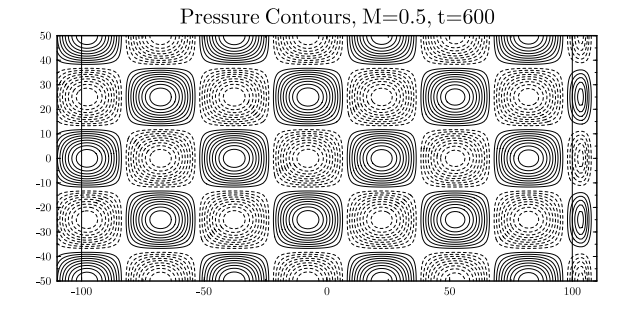


Figure 7: Propagation of a duct mode with rigid walls.

In Figure 7, we show the propagation of a twodimensional symmetric duct mode formed by an incoming wave specified as

$$\mathbf{u}_{inc} = Im \left\{ \tilde{\mathbf{f}}(y) e^{i(k_x x - \omega t)} \right\},$$

where
$$\tilde{\mathbf{f}}(y) = \begin{pmatrix} \cos(k_y y) \\ \frac{k_x}{\omega - Mk_x} \cos(k_y y) \\ \frac{ik_y}{\omega - Mk_x} \sin(k_y y) \\ \cos(k_w y) \end{pmatrix}$$
.

For the 2-D duct with rigid walls, $k_y = m\pi/50$ (where m is an integer) and $\omega = Mk_x + \sqrt{k_x^2 + k_y^2}$.

For the results shown in Figure 7, $k_y = 0.04\pi$, $k_x = 5k_y/6$ and M = 0.5. The computation was initiated with the duct mode occupying half of the computational domain. Specifically, at t = 0, we have

$$\mathbf{u}(x, y, 0) = Im \left\{ \tilde{\mathbf{f}}(y) e^{ik_x x} \right\} h(x),$$

where
$$h(x) = \frac{1}{2}[1 - \tanh(\frac{x}{5})].$$

The h(x) function was used so that the initial conditions would not have an abrupt front. Alternatively, the front can be placed inside the exit PML domain. Pressure contours at t=600 are shown in Figure 7. Judging by the regularity of the contours, the reflections from the two open boundaries are indeed quite small.

4.3 Duct of cylindrical cross section

For a duct of cylindrical cross section, Figure 5(bottom), the linearized Euler equations in cylindrical coordinates can be written as

$$\frac{\partial \mathbf{u}}{\partial t} + \mathbf{A} \frac{\partial \mathbf{u}}{\partial x} + \mathbf{B} \frac{\partial \mathbf{u}}{\partial r} + \frac{1}{r} \mathbf{C} \frac{\partial \mathbf{u}}{\partial \theta} + \frac{1}{r} \mathbf{D} \mathbf{u} = 0$$

where **A**, **B**, **C** and **D** are matrices with constant coefficients. The PML absorbing boundary condition can be derived very similarly to those in the rectangular coordinates, since only the σ_x term is needed inside the duct. We get

$$\begin{split} \frac{\partial \mathbf{u}}{\partial t} + \mathbf{A} \frac{\partial \mathbf{u}}{\partial x} + \mathbf{B} \frac{\partial \mathbf{u}^x}{\partial r} + \frac{1}{r} \mathbf{C} \frac{\partial \mathbf{u}^x}{\partial \theta} + \frac{1}{r} \mathbf{D} \mathbf{u}^x + \mathbf{u}^* \\ + \frac{\sigma_x M}{1 - M^2} \mathbf{A} \mathbf{u} &= 0 \end{split}$$

where

$$\mathbf{u}^x = \mathbf{u} + \sigma_x \mathbf{q}_1$$
 and $\mathbf{u}^* = \sigma_x \mathbf{u}$.

Due to the limitation of space, numerical example will not be given here.

5 Discussion and summary

We have reviewed basic ideas for the zonal techniques and the PML method for the linearized Euler equations. On the surface, the PML technique appears to be similar to the artificial damping technique reviewed in section 2.1. There are, however, important

and non-trivial distinctions. To provide a heuristic argument, let's compare the two methods when the absorption coefficient used is a constant $\sigma_x = \sigma_0$.

The acoustic wave solution of the linearized Euler equation (7) can be written as

$$\hat{\mathbf{u}} = A_1 \hat{\mathbf{e}}_a exp(\frac{i\omega\cos\phi}{1 + M\cos\phi}x + \frac{i\omega\sin\phi}{1 + M\cos\phi}y) \quad (29)$$

where $\hat{\mathbf{e}}_a = (1, \cos \phi, \sin \phi, 1)^T$ is the acoustic eigenvector of (7) and ϕ the phase angle.

The acoustic wave solution of the PML equations (15)-(16), by (24), is of the form

$$\hat{\mathbf{u}} = A_2 \hat{\mathbf{e}}_a exp(\frac{i\omega\cos\phi}{1 + M\cos\phi}x$$

$$-\frac{M+\cos\phi}{(1-M^2)(1+M\cos\phi)}\sigma_0 x + \frac{i\omega\sin\phi}{1+M\cos\phi}y). (30)$$

Here A_1 and A_2 are arbitrary constants. It is easy to see that the solution given in (30) can be matched exactly to that of the Euler equations given in (29) along any vertical interface of $x = x_0(constant)$ by adjusting constants A_2 or A_1 . This means that the acoustic waves can go through the interface transparently and without any reflection.

The artificial damping model of equation (5), on the other hand, would modify the linearized Euler equations as

$$\frac{\partial \mathbf{u}}{\partial t} + \mathbf{A} \frac{\partial \mathbf{u}}{\partial x} + \mathbf{B} \frac{\partial \mathbf{u}}{\partial y} + \sigma_0 \mathbf{u} = 0.$$
 (31)

The acoustic wave solution for (31), while keeping the same eigenvector $\hat{\mathbf{e}}_a$, will be

$$\hat{\mathbf{u}} = A_3 \hat{\mathbf{e}}_a exp(\frac{i\omega\cos\phi}{1 + M\cos\phi}x - \frac{\cos\phi}{1 + M\cos\phi}\sigma_0 x)$$

$$+\frac{i\omega\sin\phi}{1+M\cos\phi}y-\frac{\sin\phi}{1+M\cos\phi}\sigma_0y). \tag{32}$$

Along a vertical interface $x=x_0$, it is obvious that (32) can not be matched to (29) as a function of y, except for the special case of $\phi=0$ (i.e., normal incident). Consequently, reflections are generated at the interface.

In summary, we see two main issues for absorbing boundary conditions. The first is how to formulate the equations to be used in the absorbing zone that cause as little reflection as possible. The second is how to minimize the computational cost. These two issues are related. A better formulation of the absorbing boundary condition leads to a shorter and

more efficient absorbing layer. In this sense, the perfectly matched absorbing layer is the ultimate absorbing boundary condition. While the zonal techniques reviewed in Section 2 are generally applicable to the non-linear Euler and Navier-Stokes equations, the cases where the PML technique can be successfully applied are still limited at the present time. The PML technique for Computational Aeroacoustics is under active development. In addition to the linearized Euler equations with a uniform mean flow, the procedure described in Section 3 can be used to derive PML equation for non-uniform mean flows by assuming the mean flow Mach number M as a function of y(see Hu(2003) and Hasgstrom et al (2003)). Some ideas on applying PML to certain nonlinear Euler equations were presented in Hu(1996b). Clearly, more works are needed to further expand the application of PML to fully non-linear Euler and Navier-Stokes equations.

Acknowledgement: This work was supported by NASA grant NAG 1-01044.

References

- [1] Abarbanel, S. and Gottlieb, D. (1997) A mathematical analysis of the PML method, *Journal of Computational Physics*, **134**, 357-363.
- [2] Abarbanel, S., Gottlieb, D. and Hesthaven, J. S. (1999) Well-posed perfectly matched layers for advective acoustics, *Journal of Computational Physics*, 154, 266-283.
- [3] Alpert, B., Greengard, L. and Hagstrom, T. (2002) Nonreflecting Boundary Conditions for the time-dependent wave equation, *Journal of Computational Physics*, 180, 270-296.
- [4] Becache, B., Fauqueux, S. and Joly, P. (2003) Stability of perfectly matched layers, group velocities and anisotropic waves, *Journal of computational Physics*, **188**, 399-433.
- [5] Berenger, J.-P. (1994) A perfectly matched layer for the absorption of electromagnetic waves, Journal of computational Physics, 114, 185-200.
- [6] Chew, W. C. and Weedon, W. H. (1994) A 3D perfectly matched medium from modified Maxwell's equations with stretched coordinates, IEEE Microwave Opt, Technol. Lett., 7, 599-604.
- [7] Collino, F. and Monk, P. (1998) The perfectly matched layer in curvilinear coordinates, SIAM J. Sci, Comp, 19, No. 6, P. 2016.

- [8] Colonius, T., Lele, S. K. and Moin, P. (1993) Boundary conditions for direct computation of aerodynamic sound generation, AIAA Journal, 31, No. 9, 1574-1582.
- [9] Freund, J. B. (1997) Proposed inflow/outflow boundary condition for direct computation of aerodynamic sound, *AIAA Journal*, **35**, No. 4, 740-743.
- [10] Gedney, S. D. (1996) An anisotropic perfectly matched layer-absorbing medium for the truncation of FDTD lattices, *IEEE Trans. Antennas Propagation*, 44, 1630-1639.
- [11] Hagstrom, T. and Nazarov, I. (2003) Perfectly matched layers and radiation boundary conditions for shear flow calculations, AIAA paper 2003-3298.
- [12] Givoli, D. (1994) Non-reflecting boundary conditions, Journal of Computational Physics, 94, 1-29.
- [13] Hesthaven, J. S. (1998) On the analysis and construction of perfectly matched layers for the linearized Euler equations, *Journal of Computational Physics*, **142**, 129-147.
- [14] Hixon, R. (2004) Radiation and wall boundary conditions for computational aeroacoustics: A review, this issue.
- [15] Hu, F. Q. (1996a) On absorbing boundary conditions of linearized Euler equations by a perfectly matched layer, *Journal of Computational Physics*, 129, 201-219.
- [16] Hu, F. Q. (1996b) On Perfectly Matched Layer as an absorbing boundary condition, AIAA paper 96-1664.
- [17] Hu, F. Q. (2001) A stable, Perfectly Matched Layer for linearized Euler equations in unsplit physical variables, *Journal of Computational Physics*, **173**, 455-480.
- [18] Hu, F. Q. (2002) On constructing stable Perfectly Matched Layers as an absorbing boundary condition for Euler equations, AIAA paper 2002-0227.
- [19] Hu, F. Q. (2003) Solution of aeroacoustic benchmark problems by discontinuous Galerkin method and Perfectly Matched Layer for nonuniform mean flows, to appear in the proceeding of the 4th CAA Workshop on Benchmark problems, Oct. 2003.

- [20] Hu, F. Q. and Atkins, H. L. (2002) Eigensolutions analysis of the discontinuous Galerkin method with nonuniform grids. Part I: one space dimension, *Journal of Computational Physics*, 182, 516-545.
- [21] Israeli, M. and Orszag, S. A. (1981) Approximation of Radiation Boundary Conditions, *Journal of Computational Physics*, Vol. 41, 115-135.
- [22] Kosloff, R. and Kosloff, D. (1986) Absorbing boundary conditions for wave propagation problems, *Journal of Computational Physics*, **63**, 363-376.
- [23] Liu, C. and Liu, Z. (1993) High order finite difference and multigrid methods for spatially evolving instability in a planar channel, *Journal* of Computational Physics, 106, 92-100.
- [24] Petropoulos, P. (2000) Reflectionless sponge layers as absorbing boundary conditions for the numerical solution of Maxwell's equations in rectangular, cylindrical and spherical coordinates, SIAM J. Appl. Math., 60, 1037-1065.
- [25] Rai, M. M. and Moin, P. (1991) Direct numerical simulation of transition and turbulence in a spatially evolving boundary layer", AIAA paper 91-1607.
- [26] Renault, R. A. (1992) Absorbing boundary conditions, difference operators, and stability, *Journal of Computational Physics*, **102**, 236-251.
- [27] Streett, C. L. and Macaraeg, (1989) M. G. Spectral multi-domain for large-scale fluid dynamic simulations, *Applied Numerical Mathematics*, **6**, 123-139.
- [28] Ta'asan, S. and Nark, D. M. (1995) An absorbing buffer zone technique for acoustic wave propagation, AIAA paper 95-0164.
- [29] Tam, C. K. W. (1998) Advances in numerical boundary conditions for computational aeroacoustics, *Journal of Computational Acoustics*, **6**, 377-402.
- [30] Tam, C. K. W., Auriault, L and Cambulli, F. (1998) Perfectly Matched Layer as an absorbing boundary condition for the linearized Euler equations in open and ducted domains, *Journal* of Computational Physics, 144, 213-234.
- [31] Tsynkov, S. V. (1998) Numerical solution of problems on unbounded domains. A review, Applied Numerical Mathematics, 27, 465-532.

- [32] Turkel, E. and Yefet, A. (1998) Absorbing PML boundary layers for wave-like equations, *Applied Numerical Mathematics*, 27, 533-557.
- [33] Vichnevetsky, R. (1981) Propagation through numerical mesh refinement for hyperbolic equations, *Math. and Comp. in Simulation*, **23**, 344-395.
- [34] Visbal, M. R. and Gaitonde, D. V. (2001) Very high-order spatially implicit schemes for computational acoustics on curvilinear meshes, *Journal of Computational Acoustics*, 9, 1259-1286.
- [35] Wasistho, B., Geurts, B. J. and Kuerten, J. G. M. (1997) Simulation techniques for spatially evolving instability in compressible flow over a flat plate, *Computers & Fluids*, **26**, 713-739.
- [36] Zhao, L. and Cangellaris, A. C. (1996) GT-PML: generalized theory of perfectly match layers and its application to the reflectionless truncation of finite-difference time-domain grids, *IEEE Trans. Microwave Theory Tech.*, **44**, 2555-2563.